A General Solution to the Second Order J2 Contribution in a Mean Element Semianalytical Satellite Theory

Zachary Folcik[1]
53 Maynard Street Arlington MA, United States, zjfolcik@mit.edu
Paul J. Cefola[2]
State University of New York at Buffalo, Amherst, NY, United States, paulcefo@buffalo.edu

ABSTRACT

An improved accuracy model for the J2 zonal harmonic second order terms, J_2^2, in a general semi-analytical satellite theory is described. The new model is implemented as an option in the Draper Semi-analytic Satellite Theory (DSST) orbit propagator; the DSST is one of the several orbit propagators included in the Linux version of the R&D Goddard Trajectory Determination System (GTDS) program. The DSST previously modeled the first-order mean equinoctial orbital element rates and short periodic motion for the Earth's zonal and tesseral gravity harmonics. The current DSST also includes approximate models for the mean equinoctial orbit element rates and the short-periodic motion due to the J_2^2 zonal harmonic terms. However, these approximate J_2^2 models are truncated on the eccentricity. Building on the work of McClain, Zeis, Slutsky, and Fischer, we develop a method to calculate the J_2^2 mean element rates using Gauss-Kronrod numerical quadrature. This quadrature-based method has both analytical and numerical components. The open source symbolic algebra system, Maxima, operating on a Linux platform, is used to construct the analytical portion of the model. The accuracy of both the old and new J_2^2 models is demonstrated over a range of eccentricities and inclinations.

1. INTRODUCTION

The improvement of the second order J_2 modeling is motivated by the need to improve the Draper Semianalytic Satellite Theory (DSST) for eccentric orbits. In previous work, better agreement was obtained between the covariance and the uncertainty in the mean equinoctial orbital element space than the agreement obtained between the covariance and uncertainty statistics for other orbital state spaces [1]. However, the advantage of better covariance and uncertainty agreement only holds when modeling errors are minimized. Therefore, the authors sought to improve the modeling in the DSST for eccentric orbits and, concurrently, the agreement in covariance and uncertainty.

The errors due the J_2^2 zonal harmonic term vary with orbital energy, eccentricity and inclination. The errors for three orbits with varying inclination are displayed in Figure 1. The position error RMS of three orbits was computed by first writing two day ephemerides produced by Cowell using only J_2 zonal Earth gravity modeling. The Cowell ephemerides include J_2^2 effects due to the brute-force nature of such Cowell predictions. Those ephemerides were then fit using DSST and weighted least squares. DSST modeling during the least squares fit included only 1st order mean element equations and 1st order short periodics in the zonal models. Second order zonal perturbations were explicitly turned off in the the DSST model. The residuals, i.e. differences between the final DSST best-fit trajectory and the original Cowell trajectory in cartesian, ECI coordinates, were aggregated according to the standard RMS error formula, equation 1. It is interesting to note that the errors at 180 degrees are slightly larger than those a zero degrees. This asymmetry may be affected by the fitspan length for the DSST fit of the Cowell trajectories, but requires further investigation.

$$RMS_{error} = \sqrt{\frac{\sum_{i=1}^{N}(x_{1,i} - x_{2,i})^2}{N}} \tag{1}$$

[1] Zachary Folcik is currently Technical Staff at MIT Lincoln Laboratory

[2] Adjunct Professor, Department of Mechanical and Aerospace Engineering; also Consultant in Aerospace Systems, Spaceflight Mechanics, and Astrodynamics, Vineyard Haven, MA, USA.

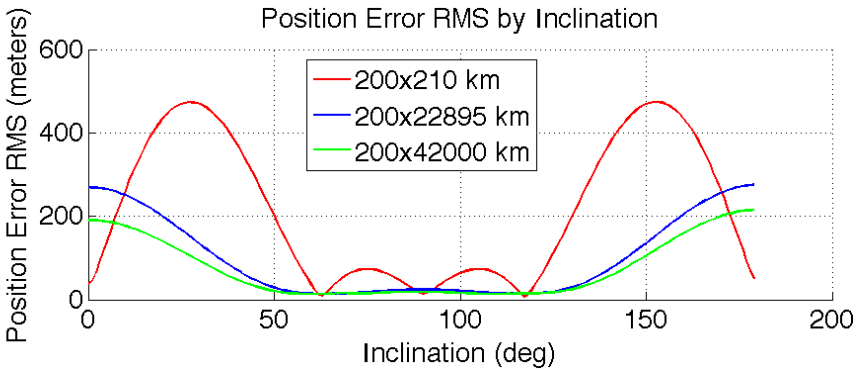

Figure 1. Position Error RMS for J_2^2 zonal harmonic perturbations for three orbits as inclination is varied. The orbits include a 200km perigee height by 210 km apogee height (near circular) orbit, a 200 km perigee height by 22895 km apogee height orbit and a 200 km perigee height by 42000 km apogee height orbit.

The errors introduced by failing to model J_2^2 are significant. For a low-altitude circular orbit at 200 km perigee height and 210 km apogee height, the errors approach 500 meters at inclinations of around 25 and 150 degrees. The errors are reduced as the apogee height is increased to 22895 km and 42000 km, but still approach 300 and 200 meters, respectively, for inclinations around zero degrees.

The first perturbation of concern when modeling the motion of an Earth satellite is J_2, the second zonal harmonic. This coefficient in the spherical harmonic expansion of Earth's gravity is roughly one thousand times larger than the next largest zonal harmonic, J_3. The J_2 coefficient is included in Blitzer's formulation of spherical harmonics for Earth's gravitational potential, U [2], [3].

$$U = -\frac{\mu}{r}\left[1 + \sum_{n=2}^{\infty}\sum_{m=0}^{n} J_{nm}\left(\frac{R_e}{r}\right)^n P_{nm}(sin\phi)cos\left(m(\lambda - \lambda_{nm})\right)\right] \tag{2}$$

Here, μ is Earth's gravitational constant, r is the distance from Earth's center of mass to the satellite, R_e is the Earth's mean equatorial radius, ϕ is the geocentric latitude, λ is the geographic longitude, and $P_{nm}sin(\phi)$ are the associated Legendre functions of the first kind of degree n and order m. The alternate formulation from [2] and [4] instead uses C_{nm} and S_{nm} coefficients.

$$U = \frac{\mu}{r}\sum_{n=2}^{\infty}\sum_{m=0}^{n}\left(\frac{R_e}{r}\right)^n P_{nm}sin(\phi)\left[C_{nm}cos(m\lambda) + S_{nm}sin(m\lambda)\right] \tag{3}$$

Variations of these spherical harmonic expansions are used in all orbit determination systems to calculate the accelerations on a satellite at a given location. In most high precision orbit determination systems, the spherical harmonics are applied at each step the integrator takes in calculating the state vector or orbital element rates. In the DSST [5], the spherical harmonic equations are embedded in the calculation of the mean element rates (zonal and tesseral resonance terms) and the short-periodic motion (zonal terms, tesseral m-daily terms, tesseral linear combination terms, and J2 secular/tesseral m-daily coupling terms). In this paper, we are specifically concerned with the treatment of the zonal spherical harmonics, and in particular the second order zonal harmonic, J_2. The DSST mean element rate equations are formulated in an asymptotic expansion allowing the separation of the contributions from any perturbation into first, second, third, etc. order mean element rate terms so only the most significant terms of interest are applied. This philosophy has allowed the theory to expand to include all first order terms and some second order terms. In the case of J_2, the first order and an approximate second order term applicable to low eccentricity orbits has previously been implemented in DSST. This paper describes the developments of a new treatment of the second order J_2, i.e. J_2^2, averaged equations of motion model in DSST which is valid for all orbital energies, eccentricities and inclinations.

The DSST has included a J_2^2 model since one was developed and implemented by Zeis and Bobick [4], [6], but this model was approximate and only intended for near-circular orbits. The errors in Figure 1 show the importance of J_2^2 for low-altitude circular orbits. If one considers the multitude

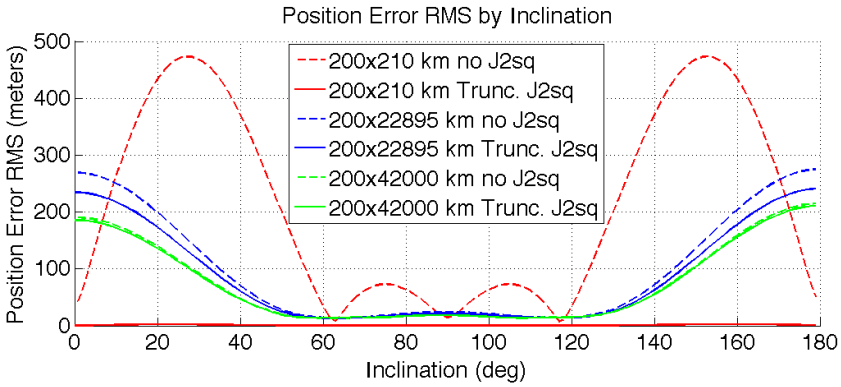

Figure 2. Position error RMS with and without the DSST truncated J_2^2 zonal harmonic perturbation model for three orbits during DSST fits of Cowell two day trajectories. Inclination is varied from zero to 180 degrees. The orbits include a 200km perigee height by 210 km apogee height (near circular) orbit, a 200 km perigee height by 22895 km apogee height orbit and a 200 km perigee height by 42000 km apogee height orbit. The Cowell trajectories include only the J_2 Earth gravity field which implicitly adds J_2^2 effects. The DSST fits of the Cowell trajectories also include only J_2 modeling, but disengage (dashed lines) or engage (solid lines) the previous, truncated, averaged element J_2^2 model.

of repeat-groundtrack, Earth observation, geosynchronous and global positioning missions, the priority of addressing effects for circular orbits is clear. Figure 2 shows the position error RMS for both the unmodeled J_2^2 perturbation cases from Figure 1 and the same cases using the truncated, approximate DSST J_2^2 perturbation model. The model effectively removes the error for the circular case. Also, the error contribution from J_2^2 is small at critical inclinations, i.e. 63.4 degrees and 116.6 degrees. This indicates that the lack of accurate J_2^2 models for critically-inclined, high eccentricity orbits such as Molniya orbits is not so important. Recent observations of low inclination, high eccentricity transfer orbits have made a complete J_2^2 model increasingly relevant, however. We note that low inclination trajectories occur naturally with launches to geosynchronous orbit from the French Guiana Space Center, the Indian launch site at Sriharikota, India, or the Hainan Island launch site that China is developing. The effect of J_2^2 at low inclination as indicated in Figures 1 and 2 drives the need for a more complete model. The relative difficulty of analytically deriving a general, closed-form J_2^2 model [2] for equinoctial elements has encumbered progress on such a model in DSST, but steady advances in computational speed for analytic and numerical approaches has eased this difficulty.

2. THE EXISTING LITERATURE

There are existing models for second order J_2 zonal harmonic effects using canonical orbital elements, namely those by Metris [7], [8], [9]. These models include closed-form solutions for J_2^2 effects.

There exist other semianalytic satellite theories that use non-canonical orbital elements, such as Semianalytic Lui Theory (SALT) [10]. This alternative semianalytic satellite theory is mainly used for satellite reentry prediction. A 1988 version of SALT includes zonal (J_2, J_3, J_4), atmospheric drag and third-body gravity models for lunar and solar point masses. Tesseral resonance, solar radiation pressure, m-daily, and second order zonal effects are not included.

DSST includes a comprehensive collection of force models to achieve better than 10 meter accuracy when fitting circular reference orbits and nearly that accuracy for eccentric orbits [2], [11]. These force models include up to 50x50 gravity fields [12], M-daily, tesseral resonance, J_2^2 for circular orbits, atmospheric drag, atmospheric density (Jacchia-Roberts, MSIS-'90 MSIS-2000), spherical and box-wing solar radiation pressure models [13], solid-Earth tides, polar motion, and lunar and solar point mass gravity. These features along with the documented history of previous, successful modifications to DSST reduce the risk in adding a complete J_2^2 model.

The work of Zeis [4], Kaniecki [14] and Fischer [2] includes the analytical development and symbolic algebra routines in the Macsyma language required to model the second order J_2 zonal harmonic. For the current effort, the authors ported this code to the current open-source incarnation of

Macsyma, i.e. Maxima [15]. However, before the details of the specific J_2^2 model are discussed, a brief overview of the general formulation for the semianalytic satellite theory applied to the second order J_2 zonal harmonic is provided for context.

3. SEMIANALYTICAL SATELLITE THEORY APPLIED TO THE SECOND-ORDER ZONAL HARMONIC

The derivation of the averaged equations of motion for a single perturbing function taken to second order in that function is summarized below. This derivation is taken from McClain [16]. The following differential equations give the rates of change of the osculating equinoctial orbital elements.

$$\frac{da_i}{dt} = \epsilon\, F_i(\boldsymbol{a}, l) \quad (i = 1, 2, 3, 4, 5) \tag{4}$$

$$\frac{dl}{dt} = n(a_1) + \epsilon\, F_6(\boldsymbol{a}, l) \tag{5}$$

Here, ϵ is a small parameter of the perturbation model which is being exercised. This small parameter, in the case of the geopotential, is a coefficient in one of the terms of the spherical harmonic expansion. In the case of this paper where the second order zonal harmonic is our focus, this small parameter is the value of J_2. The vector $\boldsymbol{a}$ includes the five slowly varying equinoctial orbital elements (a, h, k, p, q). The quantity l is the mean longitude and n is the mean motion. Mean motion in the osculating elements is related to semimajor axis, $n = \sqrt{\mu/a^3}$.

The semianalytic satellite theory distinguishes between mean or averaged elements, $(\overline{\boldsymbol{a}}, \bar{l})$, and the osculating elements, (a, l). The near identity transformation allows the transformation of mean to osculating elements and has the assumed form [16]:

$$a_i = \overline{\boldsymbol{a}}_{\boldsymbol{i}} + \sum_{j=1}^{N} \epsilon^j \eta_{i,j}(\overline{\boldsymbol{a}}, \bar{l}) + O(\epsilon^{N+1}) \quad (i = 1, 2, 3, 4, 5) \tag{6}$$

$$l = \bar{l} + \sum_{j=1}^{N} \epsilon^j \eta_{6,j}(\overline{\boldsymbol{a}}, \bar{l}) + O(\epsilon^{N+1}) \tag{7}$$

The functions, $\eta_{i,j}$ are 2π periodic in the mean longitude, l, and are often referred to as the short periodic functions. The variables with the overbar are the mean or averaged elements. The mean or averaged elements are governed by the mean element equations of motion which are assumed to have the form given by equations 8 and 9.

$$\frac{d\overline{a}_i}{dt} = \sum_{j=1}^{N} \epsilon^j A_{i,j}(\overline{\boldsymbol{a}}) + O(\epsilon^{N+1}) \quad (i = 1, 2, 3, 4, 5) \tag{8}$$

$$\frac{d\bar{l}}{dt} = n(\overline{a}_1) + \sum_{j=1}^{N} \epsilon^j A_{6,j}(\overline{\boldsymbol{a}}) + O(\epsilon^{N+1}) \tag{9}$$

Given the assumed form of the mean element equations of motion, the assumed form for the mean to osculating transformations, equations 6 and 7, and the original osculating differential equations, equations 4 and 5, we can use the Generalized Method of Averaging [16] to construct the unknown functions in equations 6, 7, 8, and 9. Equations 8 and 9 only depend on the slowly varying mean elements. Obtaining order-by-order expressions, $A_{i,j}(\overline{\boldsymbol{a}})$, for the mean element rates is detailed in [16] and yields the following equations:

$$\frac{d\overline{a}_i}{dt} = \epsilon \left\langle F_i(\overline{\boldsymbol{a}}_{\boldsymbol{i}}, \bar{l}) \right\rangle_{\bar{l}} + \epsilon^2 \left\langle \sum_{k=1}^{6} \eta_{k,1}(\overline{\boldsymbol{a}}, \bar{l}) \frac{\partial F_i(\overline{\boldsymbol{a}}, \bar{l})}{\partial \overline{a}_k} \right\rangle_{\bar{l}} + O(\epsilon^3) \quad (i = 1, 2, 3, 4, 5) \tag{10}$$

$$\frac{d\bar{l}}{dt} = \overline{n} + \epsilon \left\langle F_6(\overline{\boldsymbol{a}}, \bar{l}) \right\rangle_{\bar{l}} + \epsilon^2 \left\langle \sum_{k=1}^{6} \eta_{k,1}(\overline{\boldsymbol{a}}, \bar{l}) \frac{\partial F_6(\overline{\boldsymbol{a}}, \bar{l})}{\partial \overline{a}_k} + \frac{15}{8} \frac{\overline{n}}{\overline{a}_1^2} \eta_{1,1}^2(\overline{\boldsymbol{a}}, \bar{l}) \right\rangle_{\bar{l}} + O(\epsilon^3) \tag{11}$$

Here, the $\langle\rangle_{\bar{l}}$ symbols denote the averaging operation shown in equation 12.

$$\left\langle H(\overline{\boldsymbol{a}}, \bar{l}) \right\rangle_{\bar{l}} = \frac{1}{2\pi} \int_0^{2\pi} H(\overline{\boldsymbol{a}}, \bar{l}) d\bar{l} \tag{12}$$

The first order expressions for the mean element rates, $A_{i,1}(\overline{\boldsymbol{a}}, \bar{l})$, are independent of the short periodic functions, $\eta_{i,j}$. Because the present work concerns the mean element rates to second order, it is important to note that the second order mean element rates are not independent of the first-order short periodic functions. This fact requires an order in which to compute the mean element rate expressions, $A_{i,1}(\overline{\boldsymbol{a}})$, as shown in [16].

$$A_{i,1}(\overline{\boldsymbol{a}}) = \left\langle F_i(\overline{\boldsymbol{a}}, \bar{l}) \right\rangle_{\bar{l}} \tag{13}$$

$$A_{i,2}(\overline{\boldsymbol{a}}) = \left\langle \sum_{k=1}^{6} \eta_{k,1}(\overline{\boldsymbol{a}}, \bar{l}) \frac{\partial F_i(\overline{\boldsymbol{a}}, \bar{l})}{\partial \overline{a}_k} \right\rangle_{\bar{l}} \tag{14}$$

$$A_{6,2}(\overline{\boldsymbol{a}}) = \left\langle \sum_{k=1}^{6} \eta_{k,1}(\overline{\boldsymbol{a}}, \bar{l}) \frac{\partial F_6(\overline{\boldsymbol{a}}, \bar{l})}{\partial \overline{a}_k} + \frac{15}{8} \frac{\overline{n}(\overline{a}_1)}{\overline{a}_1^2} \eta_{1,1}^2(\overline{\boldsymbol{a}}, \bar{l}) \right\rangle_{\bar{l}} \tag{15}$$

The short periodic functions, $\eta_{i,j}(\overline{\boldsymbol{a}}, \bar{l})$, for the zonal harmonic perturbation are derived in detail in [17], [4] and [14]. The general form for the first order zonal short periodic functions is [17].

$$\eta_{i,1} = C_{i,0} + S_{i,0}(L - \lambda) + \sum_{k=1}^{5} [C_{i,k} cos(kL) + S_{i,k} sin(kL)] \tag{16}$$

Here, L is the true longitude and λ is the mean longitude of the satellite orbit. The specific form of the short periodic functions is generated by calculating the $C_{i,k}$ and $S_{i,k}$ coefficients. These calculations are detailed by Slutsky [17] and are implemented in the DSST source code. These coefficients are functions of the mean equinoctial elements (a, h, k, p, q) and of summation limits K_{max}, L_{max} and N_{max}. K_{max} is the maximum power of e^{iL}, L_{max} is the maximum power of the eccentricity, and N_{max} is the maximum power of $\frac{r}{a}$.

Several references, in addition to [16], provide detailed derivations of the DSST, i.e. details showing the progression from equations 8 and 9 to equations 10 and 11, that can be applied to any orbital perturbation including the gravitational zonal harmonics [18], [4], [19].

4. REQUIRED FUNCTIONS AND PARTIAL DERIVATIVES

The analytical development to write concise expressions for the spherical harmonic expansion in equation 3 and the $F_i(\overline{\boldsymbol{a}}, \bar{l})$ functions in equations 4 and 5 for J_2, specifically, has mostly been addressed by Zeis [4], Kaniecki [14] and Fischer [2]. The availability of computing resources since their work has enhanced the capabilities of what can be done with symbolic algebra and related computing tools. Taking advantage of those resources, the current authors consolidated the analytical development for J_2^2, corrected minor errors and applied it to writing software in DSST.

To begin, we write the $F_i(\overline{\boldsymbol{a}}, \bar{l})$ functions as defined by Cefola, [20].

$$\epsilon F_i = -\sum_{j=1}^{6} (a_i, a_j) \frac{\partial U_{2,0}}{\partial a_j} \tag{17}$$

The (a_i, a_j) expression is the set of poisson brackets for the equinoctial elements defined in [21], [22], [2], and [16].

$$(a_i, a_j) = \frac{\partial a_i}{\partial \boldsymbol{r}} \cdot \frac{\partial a_j}{\partial \dot{\boldsymbol{r}}} - \frac{\partial a_i}{\partial \dot{\boldsymbol{r}}} \cdot \frac{\partial a_j}{\partial \boldsymbol{r}} \tag{18}$$

Zeis [4] and Fischer [2] developed Macsyma routines to obtain expressions for the gravitational potential due to the second zonal harmonic, $U_{2,0}$. For the present effort, these routines were converted to Maxima routines [15] to reproduce the result.

$$U_{2,0}(a,p,q,r,L) = -\frac{J_2\, b^3\, \mu\, {R_e}^2 \left(\frac{3\left(\left(p^2-q^2\right)\, \cos(2\,L) - 2\,p\,q\, \sin(2\,L)\right)}{\left(c+1\right)^2} - \frac{c^2-4\,c+1}{2\,\left(c+1\right)^2} \right)}{a^3} \tag{19}$$

Here, $c = p^2 + q^2$ and $b = \frac{a}{r}$. The partials of $U_{2,0}$ used in equation 17 are provided by the newly ported Zeis and Fischer Maxima routines in two forms, namely **upartial.mac** and **upart2.mac**. These routines were cross-checked against each other and certain variable names were made consistent across all routines, e.g. true longitude. The **upart2.mac** routine contains explicit expressions that were derived by hand and **upartial.mac** makes use of the symbolic differentiation and algebraic capabilities of Maxima along with the **poisson.mac** routine. Numerical results indicate these parallel routines produce equivalent expressions for $\frac{\partial U_{2,0}}{\partial a_j}$ in equation 17.

In the course of reading Fischer's work, it became apparent that some partial derivative derivations included errors. For the present effort, all partial derivatives provided in Fischer's work, [2], from pages 176 to 191 (equations 5.20 through 5.79) were checked against numerical finite difference results, rework of the derivations by hand, and against symbolic results produced by Maxima. A listing of corrections to the partial derivative expressions is provided in equations 20 to 23.

Corrected equation 5.39b:

$$\dot{Y_1} = \frac{na(k + cos(L))}{\sqrt{1 - h^2 - k^2}} \tag{20}$$

Corrected equations 5.40 and 5.41:

$$\frac{\partial \left(\frac{a}{r}\right)}{\partial \lambda} = -\frac{(\frac{a}{r})^2 (ksin(L) - hcos(L))}{\sqrt{1 - h^2 - k^2}} \tag{21}$$

Corrected equations 5.51-5.53:

$$\frac{\partial \left(\frac{a}{r}\right)}{\partial k} = -\left(\frac{a}{r}\right)^2 \left[\left[\chi sinF - \beta sinF - \beta^2 \chi k(F - \lambda)\right](ksinL - hcosL) - \beta sinL(F - \lambda) - cosL\right] \tag{22}$$

Corrected equations 5.70 and 5.72:

$$\frac{\partial L}{\partial k} = \frac{a}{r}\left[sinF\left(\left(\frac{a}{r}\right)\chi^{-1}\beta + \beta\right) + \left(-\chi k\beta^2 + \left(\frac{a}{r}\right)\chi^{-1}k\beta^2 + \beta cosL\right)(\lambda - F) + sinL\right] \tag{23}$$

The preceding corrections were also made in the affected Maxima routines, **bpart2.mac** and **tlpart2.mac**.

The partials of the F_i functions required to satisfy equations 10, 11, 14 and 15 were then implemented in new Maxima routines, **write_Fpart2_f90.mac** and **write_Fpart_f90.mac**. The two routines make use of the **ffunct2.mac** and **ffunct.mac** routines which compute F_i explicitly and use the symbolic algebra features of Maxima, respectively. The partials of the F_i functions using both methods were found to be equivalent algrabraic expressions, increasing confidence in the partial derivatives. To obtain confidence in the final analytic partial derivative expressions upon implementation in the DSST Fortran source code, finite difference subroutines using the original expressions of F_i were used to check the analytic expressions for the partials of F_i. A complete listing of the Maxima routines is provided in [4] and [2]. In addition, the authors have placed the library of Maxima routines on the web [3].

[3] Dropbox share: https://www.dropbox.com/home/DSST%20J2-squared%20Model%20Enhancement

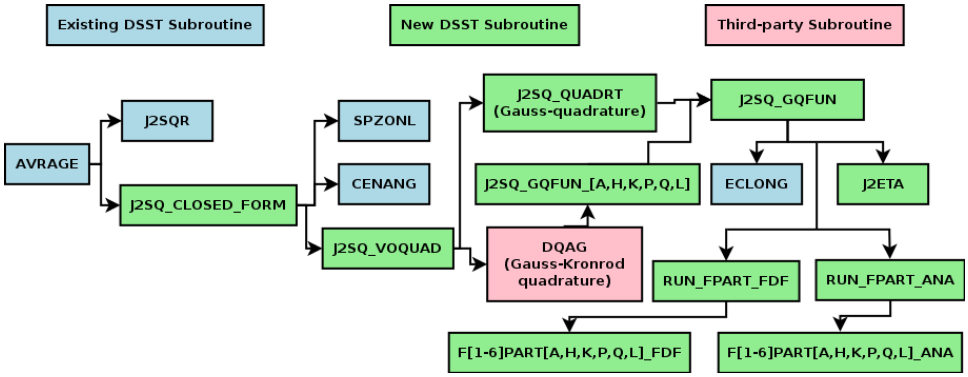

Figure 3. The calling hierarchy for the new J_2^2 model subroutines

5. IMPLEMENTATION OF A GENERAL QUADRATURE BASED J_2^2 MODEL IN DSST

The DSST implementation of a quadrature-based J_2^2 model involved writing DSST subroutines which evaluate equations 14 and 15. The subroutines needed to calculate the first-order short periodic functions, equation 16, were already available in DSST as they were developed by Slutsky, [17]. Figure 3 shows the calling hierarchy of the new J_2^2 DSST subroutines.

Because this model currently uses numerical quadrature to compute the rates due to J_2^2, it was not called from the ANAVR subroutine which directs the calculation of mean element rates for averaged potentials or short periodic generating functions that allow Lagrangian VOP. Rather, the driving subroutine for the complete J_2^2 model, J2SQ_CLOSED_FORM, was called directly from AVRAGE. AVRAGE calls other subroutines in DSST that compute rates for various perturbations of the mean equinoctial elements, including ANAVR. When development of a purely analytical formulation for mean element motion due to J_2^2 is completed, the calling sequence could be included in ANAVR. The J2SQ_VOQUAD method is called to compute the rates for the mean elements due to J_2^2. J2SQ_VOQUAD allows two quadrature methods, a Gauss quadrature applied in J2SQ_QUADRT and a Gauss-Kronrod quadrature applied using the DQAG, J2SQ_GQFUN_[A,H,K,P,Q,L] and J2SQ_GQFUN subroutines. The [A,H,K,P,Q,L] notation indicates there are six subroutines with the endings of the subroutine names listed in the brackets. The J2SQ_GQFUN subroutine used by both quadrature methods calls RUN_FPART_FDF and RUN_FPART_ANA to calculate $\partial F_i(\overline{\boldsymbol{a}}, \bar{l})/\partial \overline{a}_k$ using either finite differences or analytical expressions, respectively. In this way, the new, general DSST J_2^2 model allows two alternatives for computing the partials of the F_i functions. The F[1-6]PART[A,H,K,P,Q,L]_FDF and F[1-6]PART[A,H,K,P,Q,L]_ANA subroutines are each 36 subroutines that capture the long expressions for $\partial F_i(\overline{\boldsymbol{a}}, \bar{l})/\partial \overline{a}_k$. In this naming scheme, the [1-6] denotes the i-th function and the [A,H,K,P,Q,L] denotes the k-th element. The J2SQ_GQFUN subroutine also calls the existing DSST subroutine ECLONG to iteratively calculate the eccentric longitude required for the F_i functions and for the short periodic functions in equation 16. J2SQ_GQFUN also calls the new J2ETA subroutine which uses $C_{i,k}$ and $S_{i,k}$ coefficients computed earlier in SPZONL to calculate the values of the short periodic functions, $\eta_{i,1}$, in equation 16.

The Gauss-Kronrod quadrature method [23], [24] was added to DSST because the existing DSST Gauss quadrature method, with up to 48-point evaluations, was not sufficient to obtain the required accuracy when evaluating the integrals in equations 14 and 15. Figure 4 illustrates the point evaluations for evaluating the averaging integral from equation 14 for the semimajor axis element. The low eccentricity case performs similarly for both methods as the number of evaluation points for the Gauss-Kronrod method, 93, is about two times the number evaluated by the Gauss method, 48. The high eccentricity case, on the other hand, illustrates how the Gauss method neglects to evaluate many points around 2 radians in the mean longitude. Near 2 radians, a large change occurs near the perigee of the orbit which, if neglected, results in significant errors in the numerical evaluation of the integral. In this case the number of point evaluations for the Gauss method is also 48, but the Gauss-Kronrod method evaluates 465 points with many being in the critical region near 2 radians in mean longitude.

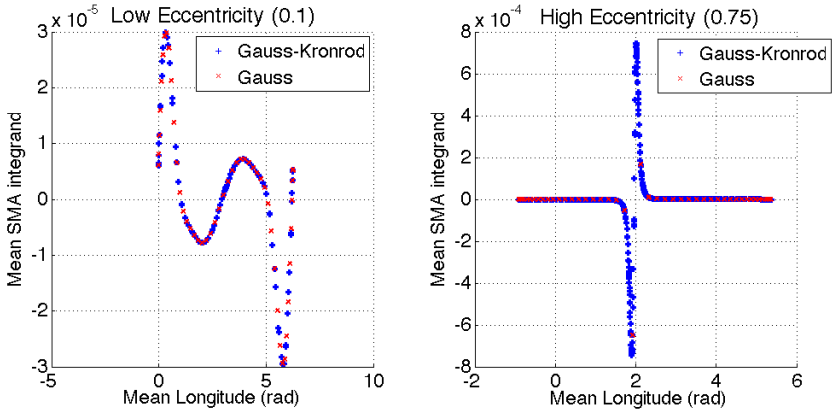

Figure 4. Point evaluations for the Gaussian and Gauss-Kronrod quadrature methods. The low-eccentricity orbit: semimajor axis = 7400 km, eccentricity = 0.1 and inclination = 45 degrees. The high-eccentricity orbit: semimajor axis = 26572 km, eccentricity = 0.75, inclination = 1.2 degrees.

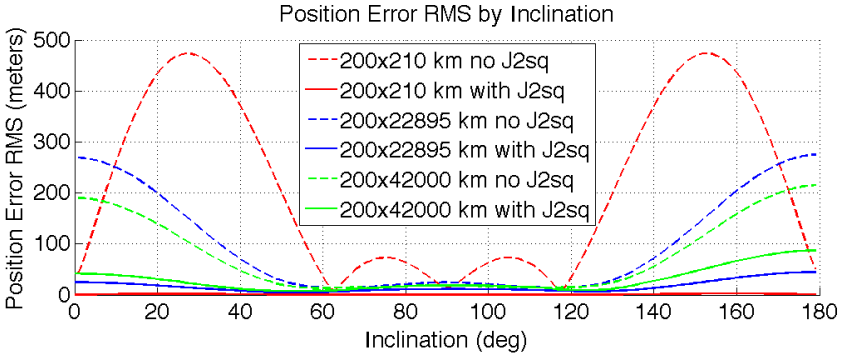

Figure 5. Position error RMS with and without J_2^2 zonal harmonic perturbations modeled for three orbits during DSST fits of Cowell two day trajectories. Inclination is varied from zero to 180 degrees. The orbits include a 200km perigee height by 210 km apogee height (near circular) orbit, a 200 km perigee height by 22895 km apogee height orbit and a 200 km perigee height by 42000 km apogee height orbit. The Cowell trajectories include only the J_2 Earth gravity field which implicitly adds J_2^2 effects. The DSST fits of the Cowell trajectories also include only J_2 modeling, but disengage (dashed lines) or engage (solid lines) the new, general, quadrature based, averaged element J_2^2 model.

6. COMPARING THE APPROXIMATE J_2^2 FORMULATION WITH THE GENERAL FORMULATION

Figure 5 shows the unmodeled J_2^2 effects for three orbits along with the errors due to higher order J_2 effects when using the new, general, quadrature based averaged element J_2^2 model. Compared to the previous J_2^2 model errors depicted in Figure 2, the quadrature based model significantly reduces the errors for the eccentric satellite cases. For the 200x22895 km orbit, the position error RMS at 180 degrees inclination was reduced from 275 meters to 45 meters. The errors with the previous model under the same test conditions were reduced from 275 meters to 241 meters. The quadrature based model also performs as well as the previous model for the circular orbit case. The position error RMS for the 200x210 km case is essentially identical, i.e. less than three meters for zero to 180 degrees inclination, using the previous and the new quadrature based J_2^2 models. The asymmetric errors due to J_2^2 at zero and 180 degrees inclination are also present in the errors when applying the quadrature based model. The remaining errors at 180 degrees inclination are somewhat larger (20 meters) than the errors at zero degrees.

Figure 6 displays position error RMS for the previous, truncated and quadrature based J_2^2 models over a grid of perigee height, apogee height and inclination values. The perigee height for both the truncated model and the quadrature based model was varied from 200 km to 2000 km in 100 km increments. The apogee height was varied from 210 km to 44010 km in 2000 km increments and the inclination was varied from zero to 150 degrees in 30 degree increments. Varying all three

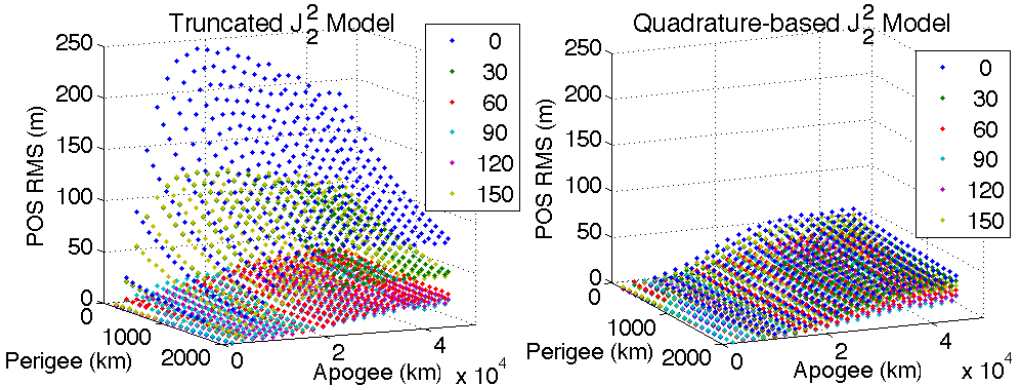

Figure 6. Position error RMS with the previous second order J2 low-eccentricity model (left plot) and the new J_2^2 general model (right plot). The position error RMS (z-axis) is shown when perigee height (x-axis), apogee height (y-axis) and inclination (legend in degrees) are varied. The original Cowell two day trajectories include only a degree and order two Earth gravity field model. This Cowell configuration includes J_2^2 implicitly. Drag, solar radiation pressure, lunar solar gravity, and Earth tide models are all turned off. The subsequent fit of the Cowell trajectories using DSST include degree and order two Earth gravity fields. The left plot shows the position error RMS results when using the DSST J_2^2 truncated model valid for low-eccentricity orbits. The right plot shows the position error RMS results when using the new, general, quadrature based, averaged element J_2^2 model.

parameters resulted in a total of 2616 position error RMS estimates. In addition to showing the significant improvement in position error with the quadrature based model, the figure illustrates a dependence on inclination. The effectiveness of both models for nearly circular orbits along the perigee axis is clear given the very small errors (all less than 3 meters). Focusing on the quadrature based model cases, the errors increase from three meters to 63 meters as the eccentricity increases from near zero to the maximum in these cases ($0 < eccentricity < 0.76986$). As the perigee increases from 200 km to 2000 km for the highest apogee cases (largest eccentricity), the errors increase from 45 meters to 63 meters. The quadrature based J_2^2 model currently calculates the mean equinoctial element rates and neglects the short periodic motion. Short periodic motion modeling should reduce these remaining errors for eccentric orbits to levels approaching the errors for circular orbits. It should be noted that the DSST short periodic model for J_2^2 which is valid only for circular orbits was engaged for all cases when J_2^2 modeling was applied in Figures 2, 5 and 6. Also, the Cowell and DSST orbit determination and predictions were made using a true equator, true equinox of reference epoch integration coordinate system.

7. CONCLUSIONS

The results of this J_2^2 modeling effort demonstrate that the completion and implementation of the mean element model developed by Zeis [4], Kaniecki [14] and Fischer [2] accurately reproduces satellite motion. Specifically, the inputs, previous work and software development needed to include equations 14 and 15 in DSST were successfully tested in the context of differential correction. This effort has helped gauge the magnitude of errors for J_2^2. The Zeis [4] satellite theory Macsyma package has been ported to the current Maxima [15] environment and the required regression testing was completed. The analytical results due to Fischer [2] were verified and extended. The DSST software now evaluates the definite integrals in equations 14 and 15 and the contribution of new Gauss-Kronrod quadrature techniques has been demonstrated. Finally, the results were only made possible by extensive testing of all analytical derivations and of many satellite orbits.

8. FUTURE WORK

Improving the computational speed of the new, complete, closed-form J_2^2 model is a high priority. Although the new model performs adequately, in terms of runtime, for propagations on the order of several days, propagations of hundreds of days require a more efficient algorithm. The first approach attempted will likely be adding capability to evaluate the averaging integrals using analytical formulae rather than the Gauss-Kronrod quadrature. Though accurate, the quadrature methods require many evaluations of the underlying functions to achieve the desired level of accuracy. Producing analytical formulae will require significant effort in decomposing the averaging

integrands. The Maxima toolset or other symbolic algebra toolsets should be useful for this effort. Currently the truncated model neglects (J2-squared x eccentricity-squared terms). One could investigate whether a model that neglects (J2-squared x eccentricity-eighth terms) might offer a compromise between accuracy and efficiency.

The larger errors due to J_2^2 effects apparent in Figures 1, 2 and 5 at 180 degrees than zero degrees inclination should be investigated. Further simulations should help determine whether this discrepancy is due to modeling or to specific test conditions such as fitspan length. Testing of the retrograde equinoctial elements should ascertain whether the prograde elements result in larger errors near 180 degrees inclination.

Solving the averaging integrals will also provide a pathway to a short-periodic model for J_2^2. The expressions for the second order short periodic functions, as given by Zeis [4], make use of the same integrands as equations 14 and 15. Decomposing these integrands is necessary to solve the short periodic functions for J_2^2 analytically.

The introduction of the Gauss-Kronrod method in DSST allows an uncomplicated way forward to replace or augment other quadrature operations in DSST. The atmosphere drag, solar radiation pressure and continuous thrust models all currently employ the existing Gauss quadrature method, but could potentially benefit from the Gauss-Kronrod method.

Currently, the quadrature based J_2^2 model has been tested with the integrator operating in true equator and equinox of reference epoch coordinates. Further modification and testing may be needed to use this model when integrating in mean equator and equinox of J2000 coordinates. Additionally, J_2-drag coupling should be considered with additional test cases. High eccentricity, long duration test cases should be analyzed with the J_2^2 model also.

The Maxima toolset offers a way to examine the properties of the Jacobi polynomials and the Hansen coefficients. This study is long overdue. A careful look at these properties is needed to better understand how to tailor DSST for high eccentricity orbits.

ACKNOWLEDGMENTS

The work of Zachary Folcik was sponsored by the Department of the Air Force under contract FA8721-05-C-0002. Opinions, interpretations, conclusions, and recommendations are those of the author and are not necessarily endorsed by the United States Government. Paul Cefola's efforts were partially supported by the University at Buffalo (SUNY) and by the Secure World Foundation. The authors ackowledge the significant contributions of Wayne McClain in developing and clearly documenting the Semianalytic Satellite Theory applied in this work. The authors are grateful for the efforts of Eric Zeis, Jean-Patrick Kaniecki, Mark Slutsky, Jack Fischer and Marty Fieger which made this work possible. The MIT Library provided electronic copies of the Zeis and Kaniecki theses. The authors thank the maintainers of the open source Maxima software. Zachary Folcik thanks Dr. Arthur Lue for suggestions and discussion of this effort. The authors thank Anye Li for prompting the authors to revisit the J_2^2 problem. Paul Cefola acknowledges his technical colleagues in the Astrodynamics community especially Prof. John Crassidis, John E. Draim (Capt. USN, ret), Dr. Dave Finkleman, Luc Maisonobe, Prof. Andrey I. Nazarenko, William Robertson (Staff Emeritus at the Draper Laboratory), Dr. Chris Sabol, Dave Vallado, Brian Weeden, Jack Wetterer, Dr. Vasiliy S. Yurasov, Martin Lara, and Juan Felix San Juan.

REFERENCES

[1] Z. Folcik, A. Lue, and J. Vatsky. Reconciling covariances with reliable orbital uncertainty. *AMOS Technology Conference and Exhibit. Maui, Hawaii.*, Sept. 2011.

[2] J.D. Fischer. The evolution of highly eccentric orbits. *Master of Science Thesis. Department of Aeronautics and Astronautics Massachusetts Institute of Technology*, June 1998.

[3] Leon. Blitzer. *Handbook of Orbital Perturbations.* University of Arizona, 1970.

[4] Eric G. Zeis. A computerized algebraic utility for the construction of nonsingular satellite theories. *Master of Science Thesis. Department of Aeronautics and Astronautics Massachusetts Institute of Technology*, Sept. 1978.

[5] P.J. Cefola, D. Phillion, and K.S. Kim. Improving access to the semianalytical satellite theory. *AAS/AIAA Astrodynamics Specialist Conference*, AAS paper 09-341, 2009.

[6] Bobick. unpublished work.

[7] G. Metris. Mean values of particular functions in the elliptic motion. *Celestial Mechanics and Dynamical Astronomy*, 52, 1991.

[8] Metris G. and Exertier P. Semi-analytical theory of the mean orbital motion. *Astronomy and Astrophysics*, 294, 1995.

[9] G. Metris and et. al. Long period variations of the motion of a satellite due to non-resonant tesseral harmonics of a gravity potential. *Celestial Mechanics and Dynamical Astronomy*, 57, 1993.

[10] W.N. Barker, S.J. Casali, and R.N. Wallner. The accuracy of general perturbations and semianalytic satellite ephemeris theories. *AAS/AIAA Astrodynamics Specialist Conference. Halifax, Nova Scotia, Canada*, AAS Paper 95-432, August 1995.

[11] S.S. Carter. Precision orbit determination from gps receiver navigation solutions. *Master of Science Thesis. Department of Aeronautics and Astronautics Massachusetts Institute of Technology*, 1996.

[12] D.J. Fonte. Implementing a 50x50 gravity field model in an orbit determination system. *Master of Science Thesis. Department of Aeronautics and Astronautics Massachusetts Institute of Technology*, 1993.

[13] R. H. Lyon. Geosynchronous orbit determination using space surveillance network observations and improved radiative force modeling. *Master of Science Thesis. Department of Aeronautics and Astronautics Massachusetts Institute of Technology*, June 2004.

[14] Jean-Patrick Rene Kaniecki. Short periodic variations in the first-order semianalytical satellite theory. *Master of Science Thesis. Department of Aeronautics and Astronautics Massachusetts Institute of Technology*, Sept. 1979.

[15] Maxima, a computer algebra system. url: http://maxima.sourceforge.net/documentation.html, July 2012.

[16] W.D. McClain. A recursively formulated first-order semianalytic artificial satellite theory based on the generalized method of averaging (the blue book). *Computer Sciences Corporation CSC/TR-77/6010 [in 1992, Wayne Mclain updated the blue book. This revised version has been scanned and is available as an electronic document]*, Volume 1, 1977.

[17] M. Slutsky. Zonal harmonic short-periodic model developed for the precision orbit propagation (pop) contract. *Draper Laboratory Memorandum PL-016-81-MS*, 30 Nov 1981.

[18] A.J. Green. Orbit determination and prediction processes for low altitude satellites. *Doctor of Philosophy Thesis. Department of Aeronautics and Astronautics Massachusetts Institute of Technology*, December 1979.

[19] Z. Folcik. Orbit determination using modern filters/smoothers and continuous thrust modeling. *Master of Science Thesis. Department of Aeronautics and Astronautics Massachusetts Institute of Technology*, June 2008.

[20] P.J. Cefola and W.D. McClain. A recursive formulation of the short-periodic perturbations in equinoctial variables. *AAS/AIAA Astrodynamics Specialist Conference. Palo Alto, California*, AAS Paper 78-1383, Aug. 7-9, 1978.

[21] R.A. Broucke and P.J. Cefola. On the equinoctial orbital elements. *Celestial Mechanics*, Volume 5 Issue 3, 1972.

[22] D.A. Danielson and et. al. Semianalytic satellite theory (SST): Mathematical algorithms. *Naval Postgraduate School*, Report Number NPS-MA-94-001, Jan. 1994.

[23] D. Kahaner, C Moler, and S. Nash. *Numerical Methods and Software*. Englewood Cliffs NJ: Prentice Hall, 1989.

[24] R. Piessens and E. De Doncker. Quadpack. url: http://www.netlib.org/quadpack, July 2012.